Electronic Supporting Information (ESI) for:

Manipulating the D:A Interfacial Energetics and Intermolecular Packing for 19.2% Efficiency Organic Photovoltaics†

Chengliang He,[a] Youwen Pan,[a] Yanni Ouyang,[b] Qing Shen,[a] Yuan Gao,[c] Kangrong Yan,[a] Jin Fang,[d] Yiyao Chen,[e] Chang-Qi Ma,[d] Jie Min,[c] Chunfeng Zhang,[b] Lijian Zuo*[a] and Hongzheng Chen*[a]

[a] State Key Laboratory of Silicon Materials, MOE Key Laboratory of Macromolecular Synthesis and Functionalization, International Research Center for X Polymers, Department of Polymer Science and Engineering, Zhejiang University, Hangzhou 310027, P. R. China. *E-mail: zjuzlj@zju.edu.cn, hzchen@zju.edu.cn.

[b] National Laboratory of Solid-State Microstructures, School of Physics, and Collaborative Innovation Center for Advanced Microstructures, Nanjing University, Nanjing 210093, P. R. China.

[c] The Institute for Advanced Studies, Wuhan University, Wuhan 430072, P. R. China.

[d] *i*-Lab & Printable Electronics Research Centre, Suzhou Institute of Nano-tech and Nano-bionics, Chinese Academy of Sciences, Suzhou 215123, P. R. China.

[e] Vacuum Interconnected Nanotech Workstation (Nano-X), Suzhou Institute of Nano-Tech and Nano-Bionics, Chinese Academy of Sciences, Suzhou 215123, P. R. China.

Table of Contents

1. Materials Synthesis

All reagents and solvents, unless otherwise specified, were purchased from commercial sources and were used without further purification. PM6 was purchased from Solarmer Material Inc. L8-BO was purchased from Guangzhou ChasingLight Technology Co., Ltd. BTP-2CHO and F-INCN, Cl-INCN, Br-INCN were purchased from Nanjing Zhiyan Technology Co., Ltd.

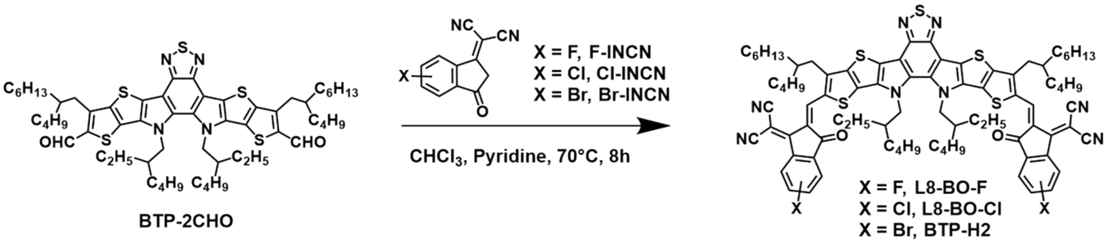

Scheme S1 Synthetic route for L8-BO-F, L8-BO-Cl and BTP-H2.

Synthesis of BTP-H2

To a Schlenk tube were added BTP-2CHO (150 mg, 0.14 mmol), Br-INCN (120 mg, 0.44 mmol), and dried $CHCl_3$ (40mL). Then the mixture was frozen by liquid nitrogen, after vacuum and Ar circulated for three times, 0.5 mL pyridine was added. The mixture was refluxed at 70 °C for 8 h. After removing the solvent, silica gel column chromatography was used to purify the product with the mixture of dichloromethane and petroleum ether (1.5:1~2:1, v/v) as the eluent, yielding a black solid (184 mg, 82%). L8-BO-F and L8-BO-Cl were synthesised by the same procedure mentioned above.

BTP-H2 ^{1}H NMR (500 MHz, $CDCl_3$, δ): 9.15 (s, 2H), 8.83 and 8.56-8.54 (m, 2H), 8.04 and 7.82-7.75 (m, 2H), 7.93-7.82 (m, 2H), 4.89-4.67 (m, 4H), 3.27-3.05 (m, 4H), 2.20-1.99 (m, 4H), 1.50-1.42 (m, 4H), 1.42-1.11 (m, 32H), 1.10-0.90 (m, 12H), 0.89-0.80 (m, 12H), 0.80-0.72 (m, 6H), 0.71-0.60 (m, 6H).

L8-BO-F ^{1}H NMR (500 MHz, $CDCl_3$, δ): 9.16 (s, 2H), 8.75 (dd, J = 3.4 Hz, J = 3.6 Hz, 0.63H), 8.41 (dd, J = 1.6 Hz, J = 5.6 Hz, 1.32H), 7.96 (dd, J = 4.2 Hz, J = 2.4 Hz, 1.33H), 7.59 (dd, J = 2.0 Hz, J = 3.3 Hz, 0.63H), 7.46-7.39 (m, 2H), 4.91-4.65 (m, 4H), 3.33-3.03 (m, 4H), 2.15-2.04 (m, 4H), 1.51-1.43 (m, 4H), 1.40-1.16 (m, 32H), 1.10-0.93 (m, 12H), 0.88-0.81 (m, 12H), 0.78-0.73 (m, 6H), 0.68-0.63 (m, 6H).

L8-BO-Cl ^{1}H NMR (500 MHz, $CDCl_3$, δ): 9.15 (s, 2H), 8.67 (d, J = 1.2 Hz, 1.04H), 8.64 (d, J = 6.7 Hz, 0.78H), 7.89-7.83 (m, 2H), 7.74-7.64 (m, 2H), 4.88-4.68 (m, 4H), 3.16 (d, J = 5.9 Hz, 4H), 2.16-2.02 (m, 4H), 1.50-1.43 (m, 4H), 1.38-1.17 (m, 32H), 1.09-0.93 (m, 12H), 0.88-0.81 (m, 12H), 0.79-0.74 (m, 6H), 0.69-0.62 (m, 6H).

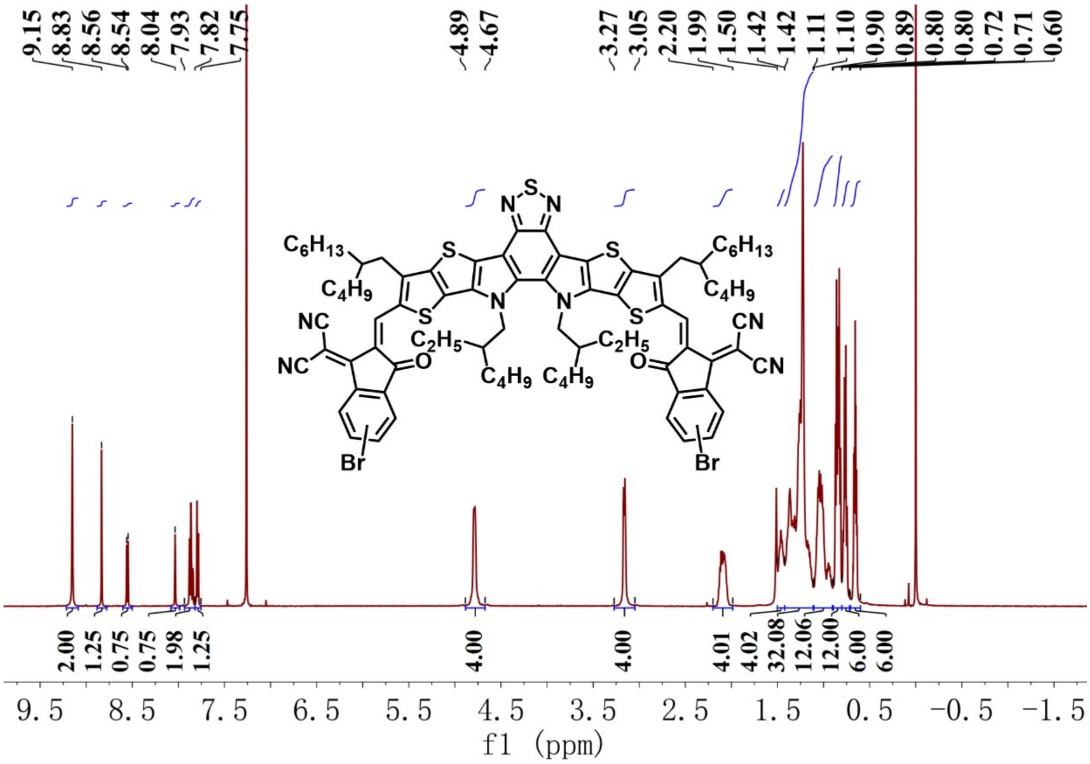

Fig. S1 NMR spectrum of BTP-H2.

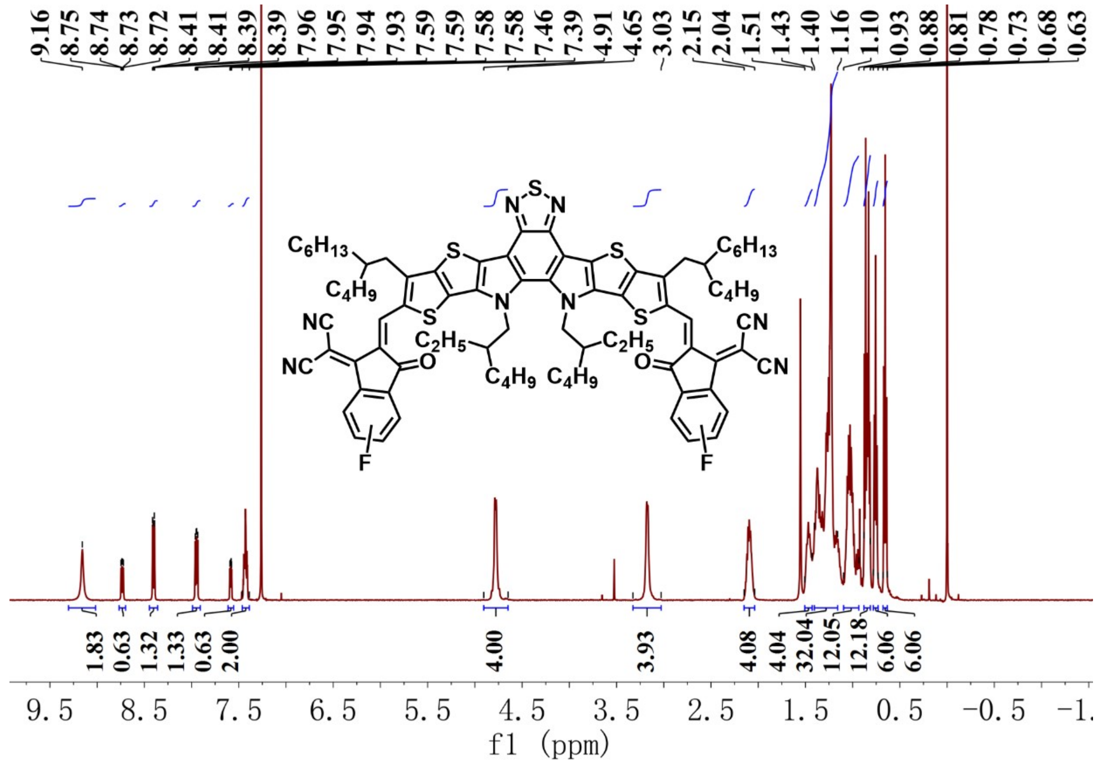

Fig. S2 NMR spectrum of L8-BO-F.

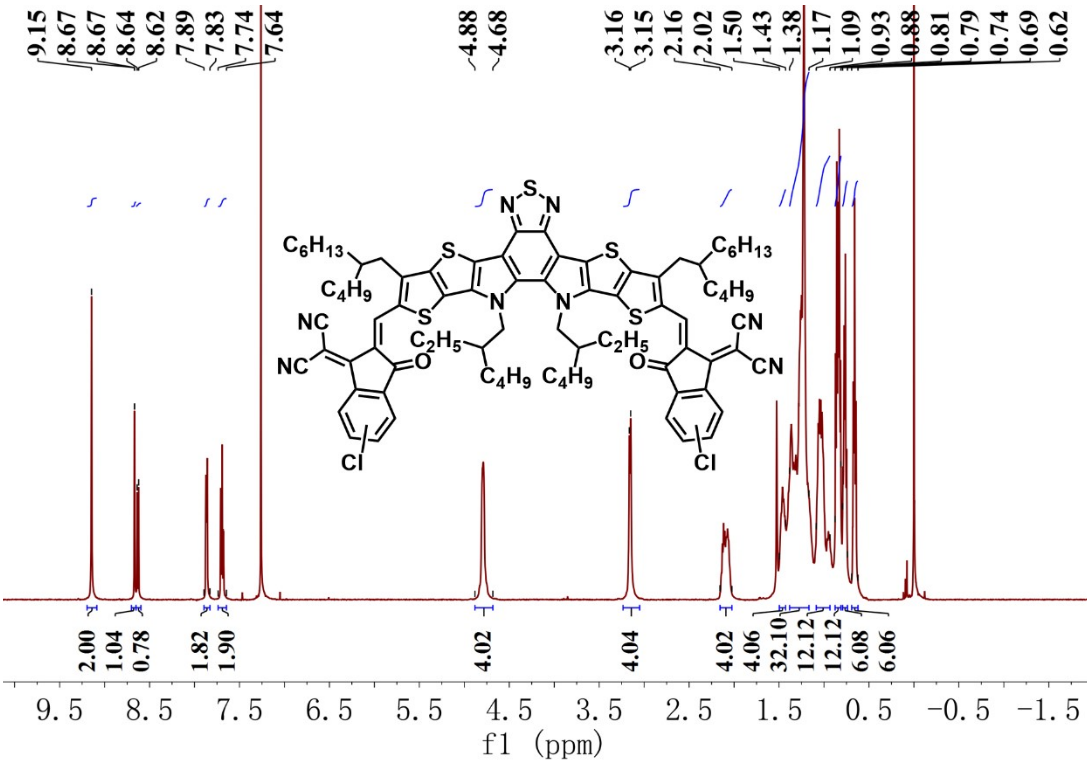

Fig. S3 NMR spectrum of L8-BO-Cl.

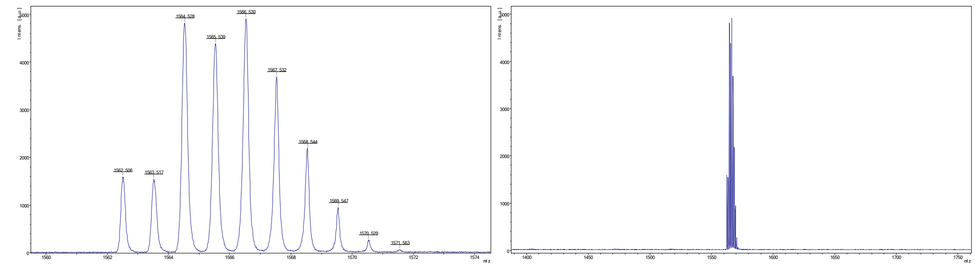

Fig. S4 High-resolution mass spectra of BTP-H2.

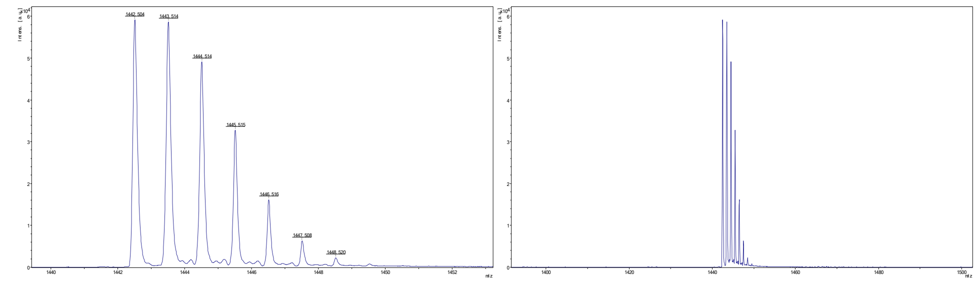

Fig. S5 High-resolution mass spectra of L8-BO-F.

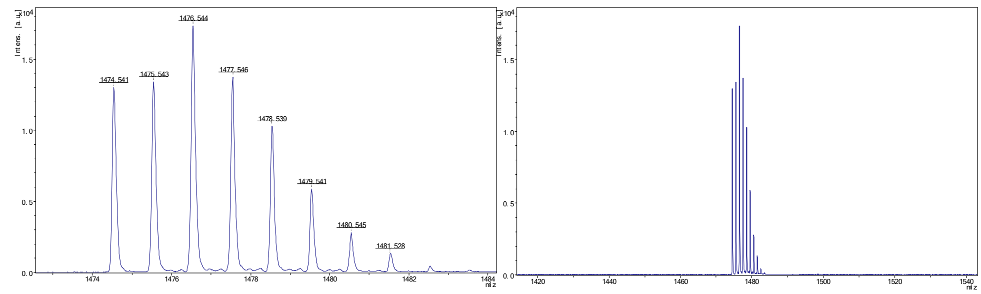

Fig. S6 High-resolution mass spectra of L8-BO-Cl.

Note: [1]H NMR tests were carried out with a Bruker Advance 500 (500 MHz) NMR spectroscope. Matrix-assisted laser desorption/ionization time of flight (MALDI-TOF) MS spectrum was obtained on the Bruker Ultraflex MALDI.

2. UV-vis Absorption Spectroscopy

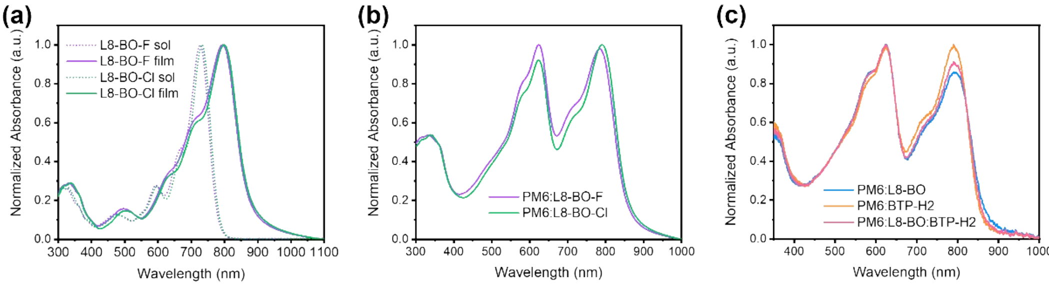

Fig. S7 Normalized absorption spectra of (a) pristine acceptors and (b, c) the blend films.

Note: UV-vis absorption spectra were measured on a Shimadzu UV-1800 spectrophotometer.

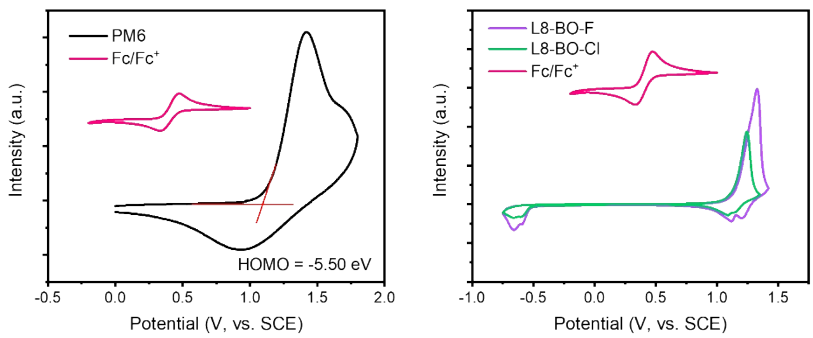

3. Cyclic Voltammetry (CV)

Fig. S8 Cyclic voltammogram of the polymer donor (PM6) and the acceptors (L8-BO-F and L8-BO-Cl).

Note: Cyclic voltammetry was done on a CHI600A electrochemical workstation by utilizing the acetonitrile solution of 0.1 mol/L tetrabutylammoniumhexafluorophosphate (Bu_4NPF_6). The CV curves were recorded versus the potential of SCE, which was calibrated by the ferrocene-ferrocenium (Fc/Fc^+) redox couple (4.8 eV below the vacuum level). Then LUMO and HOMO levels was calculated by the equation of $E_{LUMO/HOMO} = -e\ (E_{red/ox}+4.41)$ (eV).

4. Device Performance

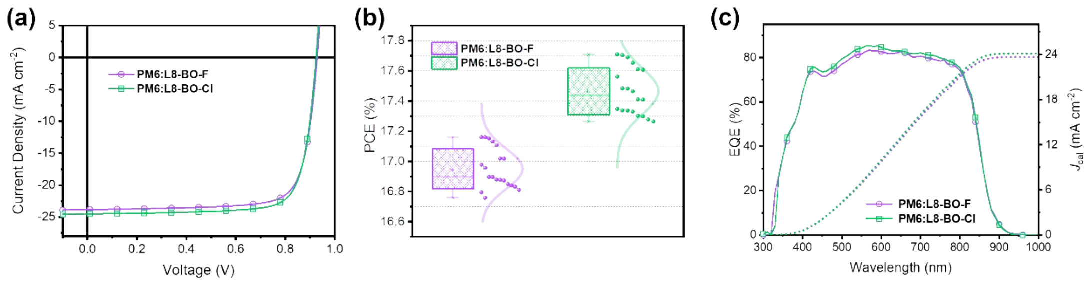

Fig. S9 (a) *J-V* curves of the optimal devices. (b) PCE statistics of 20 cells for each blend. (c) EQE curves of the optimal devices.

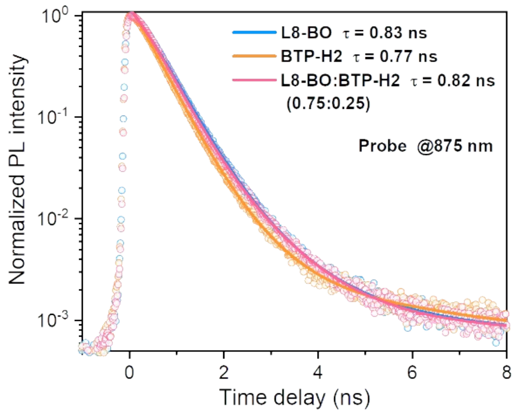

5. Time-resolved Photoluminescence Measurement

Fig. S10 Time-resolved photoluminescence spectra of L8-BO, BTP-H2 and L8-BO:BTP-H2 thin films probed at 875 nm.

6. Femtosecond Transient Absorption Spectroscopy

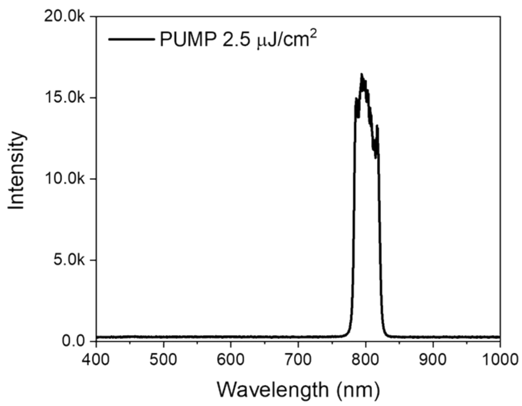

Fig. S11 Pump pulses adopted for selective excitations of acceptors for transient absorption measurements.

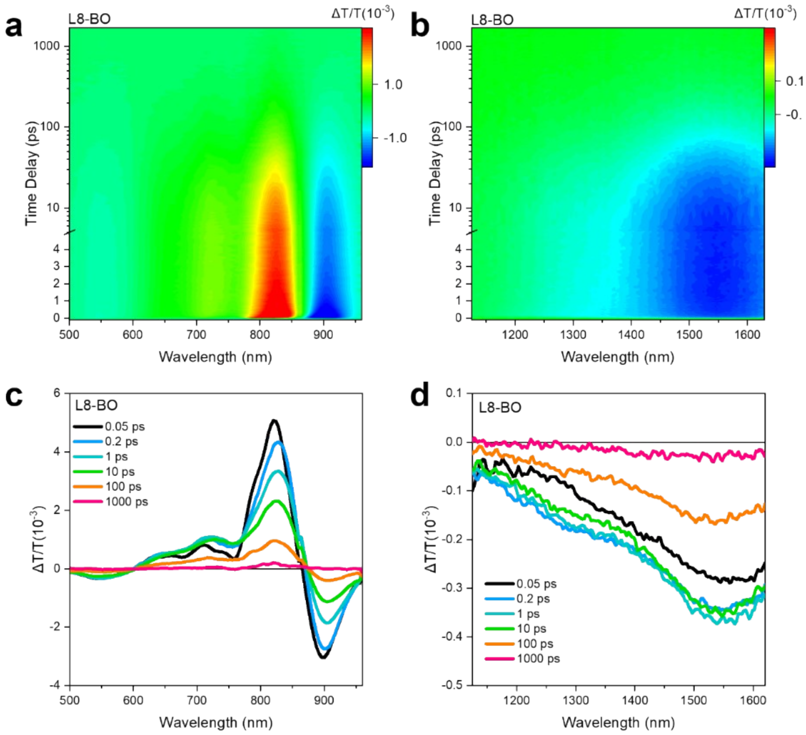

Fig. S12 (a, b) Color plots of the TA spectra of the L8-BO film at around 800 nm excitation. (c, d) TA spectra of the pristine L8-BO film at different delay times.

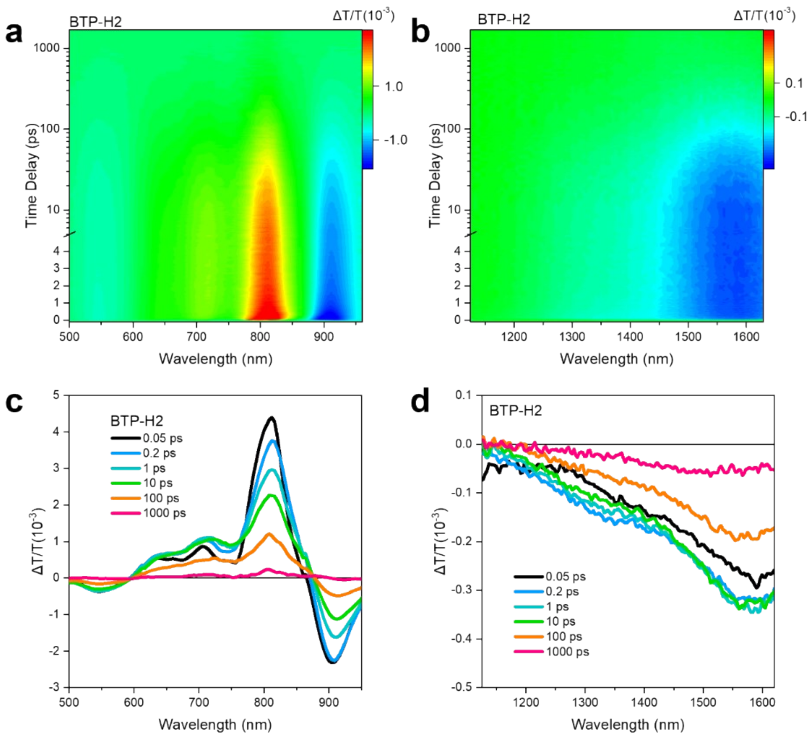

Fig. S13 (a, b) Color plots of the TA spectra of the BTP-H2 film at around 800 nm excitation. (c, d) TA spectra of the pristine BTP-H2 film at different delay times.

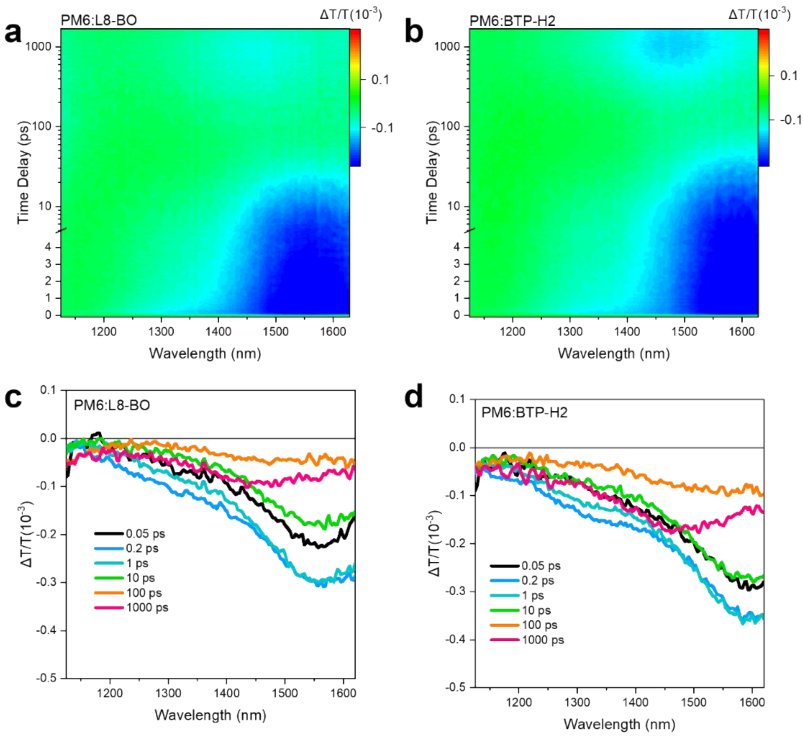

Fig. S14 (a, b) Color plots of the TA spectra of the PM6:L8-BO blend and PM6:BTP-H2 blend at around 800 nm excitation. (c, d) TA spectra of the PM6:L8-BO blend and PM6:BTP-H2 blend at different delay times.

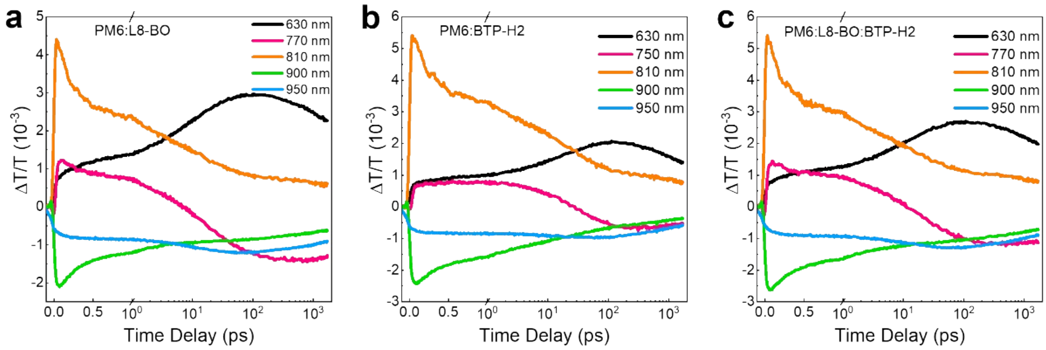

Fig. S15 TA traces of the three blends probed at different wavelengths.

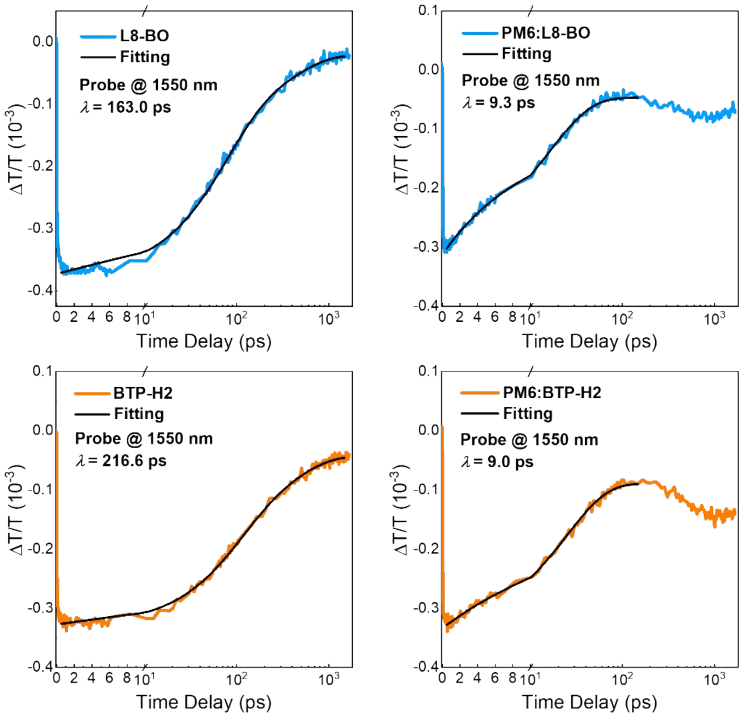

Fig. S16 TA traces of the pristine films and blend films for L8-BO and BTP-H2 probed at 1550 nm.

Note: We extract the value of hole transfer efficiency (η_{HT}) from the TA data by the following methods: first, the rate of hole transfer is estimated by the different decay rates of the excited states in the neat acceptor and the blend films, i.e., $k_{\text{i-EX}\to\text{G}} = 1/\lambda_1$, $k_{HT} = 1/\lambda_2 - 1/\lambda_1$, where $k_{\text{i-EX}\to\text{G}}$ is the i-EX decay rate, k_{HT} is the hole transfer rate, λ_1 and λ_2 are the lifetimes probed at 1550 nm in the neat and blend films (**Fig. S16**). If we consider the i-EX lifetime shortening is solely contributed by hole transfer, the quantum efficiency is thus calculated as $\eta_{HT} = k_{HT}/(k_{HT} + k_{\text{i-EX}\to\text{G}}) = 1 - \lambda_2/\lambda_1$.

7. Energy Loss Calculation

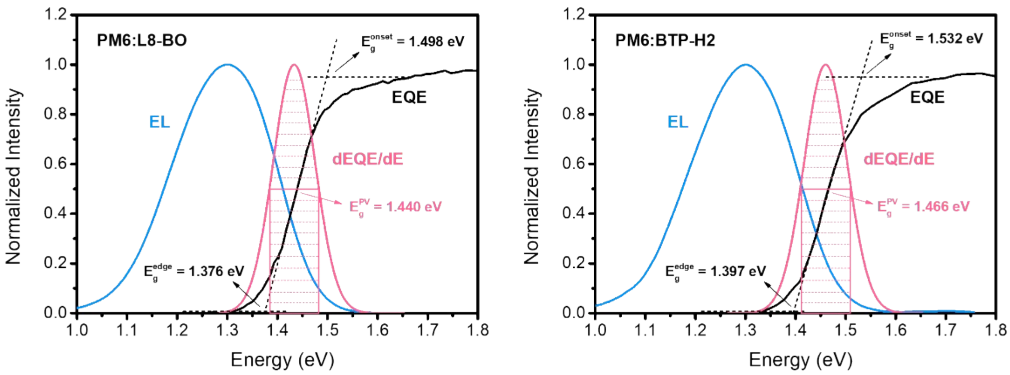

Fig. S17 E_g determination method.

Note: The total energy loss (E_{loss}) can be attributed to three parts following Equation

$$\begin{aligned} E_{loss} &= E_g - qV_{oc} \\ &= (E_g - qV_{oc}^{SQ}) + (qV_{oc}^{SQ} - qV_{oc}^{rad}) + (qV_{oc}^{rad} - qV_{oc}) \\ &= (E_g - qV_{oc}^{SQ}) + q\Delta V_{oc}^{rad,below\ gap} + q\Delta V_{oc}^{non-rad} \\ &= \Delta E_1 + \Delta E_2 + \Delta E_3 \end{aligned}$$

below:

where E_g is the bandgap, q is the elementary charge, V_{oc}^{SQ} is the maximum voltage based on the Shockley-Queisser limit (SQ limit), V_{oc}^{rad} is the open-circuit voltage when there is only radiative recombination, $\Delta V_{oc}^{rad,below\ gap}$ is the voltage loss of radiative recombination from the absorption below the bandgap and $\Delta V_{oc}^{non-rad}$ is the voltage loss of non-radiative recombination. ΔE_1 is due to radiative recombination from the absorption above the bandgap, ΔE_2 is due to radiative recombination from the absorption below the bandgap and ΔE_3 is due to non-radiative recombination. The third part, non-radiative loss, could be directly calculated by Equation :

$$\Delta E_3 = q\Delta V_{oc}^{non-rad} = -kT\ln(EQE_{EL})$$

where k is the Boltzmann constant, T is temperature and EQE_{EL} is radiative quantum efficiency of the OSCs when charge carriers are injected into the device in the dark.

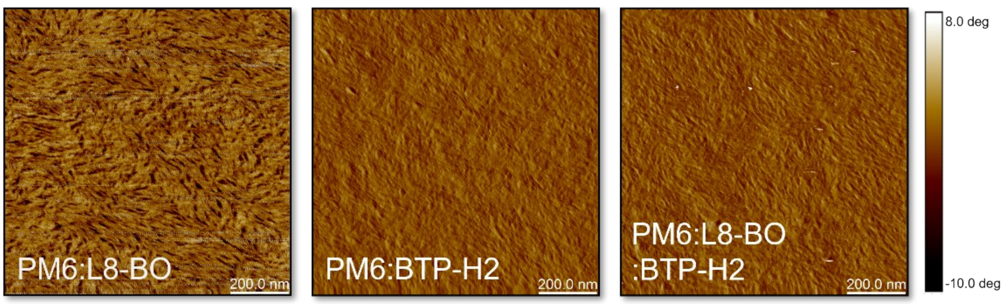

8. Morphology Investigation

Fig. S18 AFM phase images of the three blend films.

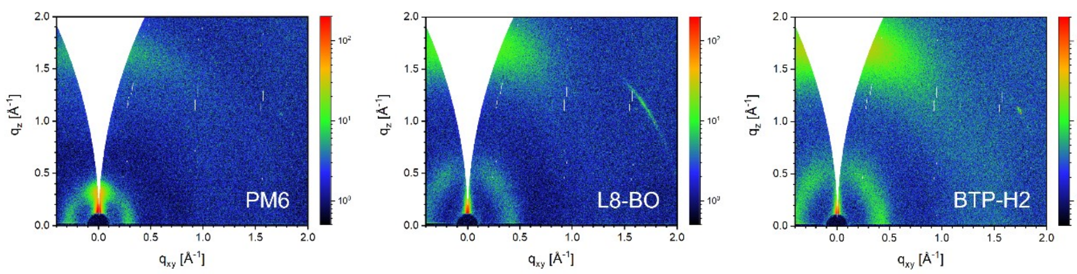

Fig. S19 2D GIWAXS images of pristine donor/acceptor films.

9. Certification Test Report

福建省计量科学研究院
FUJIAN METROLOGY INSTITUTE
（国家光伏产业计量测试中心）
National PV Industry Measurement and Testing Center

中国认可
国际互认
检测
TESTING
CNAS L0131

检 测 报 告
Test Report

报告编号：22Q3-00029
Report No.

客户名称 Name of Customer	Zhejiang University
联络信息 Contact Information	Zhejiang University, No. 38 Yugu Road, Hangzhou, Zhejiang Province, P. R. China
物品名称 Name of items	Organic Solar Cells
型号/规格 Type /Specification	1.5cm × 1.5cm
物品编号 Items No	PM6:L8-BO:BTP-H2
制造厂商 Manufacturer	Department of Polymer Science & Engineering, Zhejiang University
物品接收日期 Items Receipt Date	2022-01-29
检测日期 Test Date	2022-01-29

福建省计量科学研究院 证书/报告专用章 35010200564034

批准人 Approved by	黎健生	黎健生
核验员 Checked by	何翔	何翔
检测员 Test by	陈彩云	陈彩云

发布日期 Date of Report 2022 年 Year 02 月 month 08 日 Day

扫一扫 查真伪

本院/本中心地址：福州市屏东路 9-3 号 Address : 9-3 Pingdong Road.Fuzhou.China
电话：0591-87845050 Telephone
传真：0591-87808417 Fax
邮编：350003 Post Code
网址：www.fjjl.net Web Site
咨询电话：0591-87845050 Inquire line
投诉电话：0591-87823025 Complaint Tel

第 1 页/共 7 页
Page of Pages

1. 检测机构说明：
Testing institutions that

本院为国家法定计量检定机构，国家光伏产业计量测试中心依托本院检测技术开展检测。本院/本中心质量管理体系符合 GB/T 27025（ISO/IEC 17025，IDT）标准要求。

The institute is a national legal metrological institution. National PV Industry Measurement and Testing Center carrys out testing relying on the institute's testing technology. The Center's quality management system meets the requirements of GB/T 27025（ISO/IEC 17025，IDT）standard.

2. 本次检测所依据的检测方法（代号及名称）：
Reference documents from the test (code.name)

IEC 60904-1-2020 光伏器件-第一部分：光伏电流-电压特性的测量;IEC 60904-8:2014 光伏器件-第 8 部分光伏器件的光谱响应度测量

3. 本次检测所使用的主要测量仪器：
Measurement standards used in this test

仪器名称 Name	仪器编号 Number	测量范围 Measuring Range	不确定度/或准确度等级/或最大允许误差 Uncertainty or Accuracy Class or Maximum Permissible Error	溯源机构名称/证书编号 Name of traceability institution/Certificate No.	有效期限 Due date
系统源表（电子负载）	4082810	100 nA～3 A；(0.1～40) V	U_{rel}=0.005% (k=2)	上海市计量院 2021F11-10-3083069001	2022-03-10
太阳模拟器	2015-006	(300～1200) nm；(800～1200) W/m^2	光谱匹配度：(300～310) nm：U_{rel}=7.4% (k=2);(310～400) nm：U_{rel}=6.4% (k=2);(400～1200) nm：U_{rel}=5.5% (k=2); 辐照度比：U_{rel}=1.2% (k=2)	福建计量院 21Q2-00682	2022-06-28
WPVS 单晶硅标准电池	015-2014	(300～1200) nm	U_{rel}=1.3% (k=2)	中国计量院 GXgf2021-10725	2023-04-05
Si 光电探测器	Si-2	(200~1100)nm	(300～450) nm U_{rel}=1.8%～1.3% (k=2)；(450～1000) nm U_{rel}=1.2%～1.7% (k=2)	中国计量院 GXgf2021-10903	2023-03-24
数字温度计	15-B	(15～65)℃	U=0.1% (k=2)	福建计量院 21B2-08012	2022-06-22

4. 检测地点及环境条件：
Location and environmental condition for the test

地点：Room 108, Building 4, MinHou Scientific Research Base
Location

温度：24.5 ℃ 相对湿度：48 % 其它：/
Temperature Relative Humidity Others

5. 备注：/
Note

检测结果/说明：
Results of Test and additional explanation.

1 Standard Test Condition (STC)：Total Irradiance：1000 W/m^2
Temperature：25.0 ℃
Spectral Distribution：AM1.5G

2 Measurement Data and I-V/P-V Curves under STC

Forward Scan

I_{sc} (mA)	V_{oc} (V)	I_{MPP} (mA)	V_{MPP} (V)	P_{MPP} (mW)	FF (%)	η (%)
1.235	0.8920	1.143	0.7679	0.8777	79.67	18.77

Reverse Scan

I_{sc} (mA)	V_{oc} (V)	I_{MPP} (mA)	V_{MPP} (V)	P_{MPP} (mW)	FF (%)	η (%)
1.235	0.8916	1.143	0.7679	0.8780	79.74	18.78

Mismatch factor: 0.9941

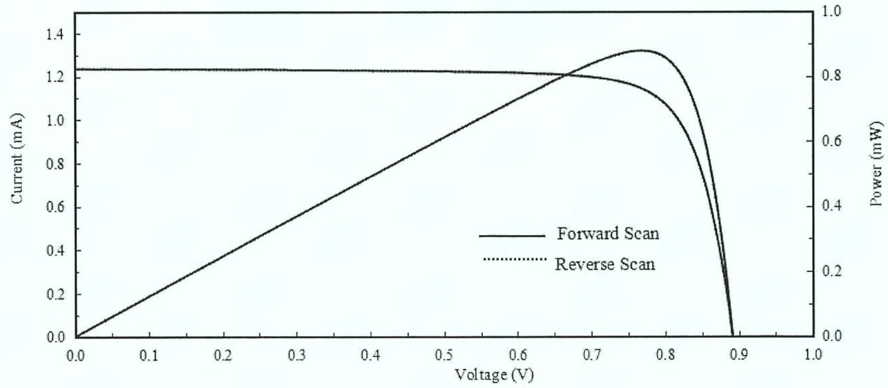

Figure 1. I-V and P-V characteristic curves of the measured sample under STC

检测结果/说明：
Results of Test and additional explanation.

3 Measurement Data and Curve of Relative Spectral Responsivity (SR) of the Measured Sample

Wavelength (nm)	SR(%)	Wavelength (nm)	SR(%)	Wavelength (nm)	SR(%)	Wavelength (nm)	SR(%)	Wavelength (nm)	SR(%)
300	0.19	445	52.93	590	81.65	735	98.97	880	31.83
305	0.20	450	53.91	595	82.40	740	99.22	885	26.39
310	0.65	455	54.73	600	82.97	745	99.28	890	22.64
315	1.51	460	55.53	605	83.40	750	99.41	895	18.31
320	2.70	465	56.47	610	83.46	755	99.33	900	14.71
325	4.20	470	57.46	615	83.62	760	99.24	905	11.81
330	5.84	475	58.54	620	83.92	765	99.32	910	9.23
335	7.49	480	59.65	625	84.22	770	99.64	915	7.19
340	9.06	485	60.77	630	84.68	775	99.79	920	5.33
345	10.46	490	61.92	635	84.98	780	99.90	925	4.22
350	11.73	495	63.10	640	85.63	785	100.00	930	3.24
355	12.97	500	64.32	645	86.09	790	99.94	935	2.50
360	14.14	505	65.59	650	86.49	795	99.70	940	1.93
365	15.38	510	66.80	655	87.36	800	99.31	945	1.52
370	16.54	515	68.12	660	88.41	805	98.62	950	1.20
375	17.82	520	69.36	665	89.44	810	97.56	955	0.94
380	19.34	525	70.52	670	90.51	815	96.24	960	0.75
385	21.27	530	71.64	675	91.70	820	94.67	965	0.60
390	23.66	535	72.71	680	92.66	825	92.64	970	0.47
395	26.41	540	73.81	685	93.56	830	90.76	975	0.37
400	29.44	545	74.81	690	94.33	835	87.87	980	0.28
405	32.85	550	75.89	695	95.05	840	83.80	985	0.21
410	36.41	555	76.82	700	95.66	845	79.00	990	0.19
415	39.90	560	77.62	705	96.31	850	73.28	995	0.14
420	43.10	565	78.38	710	96.83	855	66.31	1000	0.10
425	45.91	570	78.99	715	97.35	860	59.37	/	/
430	48.31	575	79.56	720	97.91	865	52.15	/	/
435	50.23	580	80.16	725	98.33	870	45.01	/	/
440	51.75	585	80.85	730	98.66	875	38.25	/	/

检测结果/说明：
Results of Test and additional explanation.

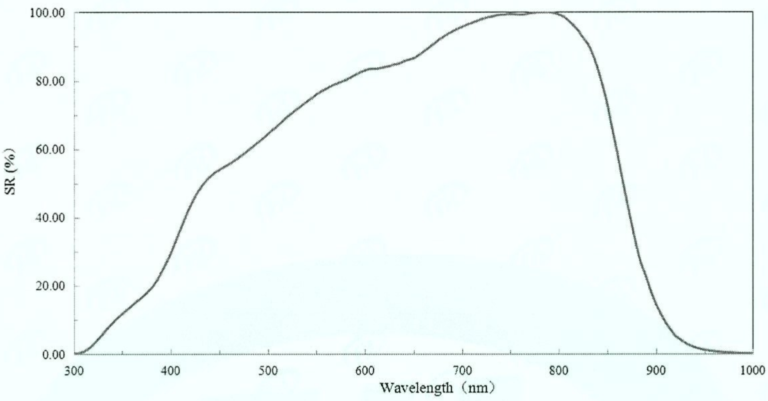

Figure 2. Relative spectral responsivity curve of the measured sample

4 Pictures of the Measured Sample

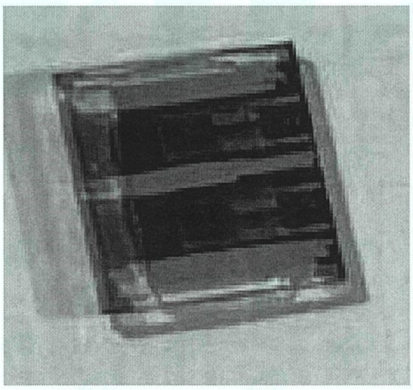

Figure 3. Obverse side of the measured sample

检测结果/说明：
Results of Test and additional explanation.

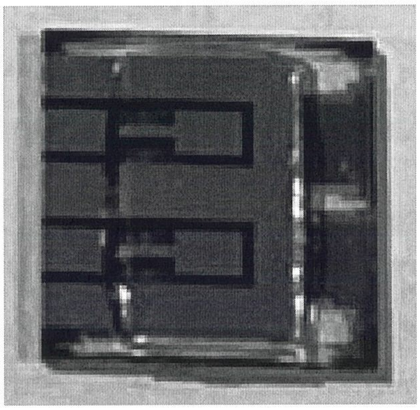

Figure 4. Reverse side of the measured sample

Uncertainty of measurement results:

Short-Circuit Current: U_{rel}=1.4% (k=2); Open-Circuit Voltage: U_{rel}=1.0% (k=2);

Maximum Power: U_{rel}=2.2% (k=2); Efficiency: U_{rel}=2.2% (k=2); Fill Factor: U_{rel}=3.2% (k=2).

Relative Spectral Responsivity:

(300~400) nm: U_{rel} = 2.2% (k=2);

(400~1000) nm: U_{rel} = 1.8% (k=2).

说明：The effective area of the measured sample was 0.04675 cm^2.
Explanation

Testing method (code and name) for this test
IEC 60904-1: 2020 Photovoltaic devices- Part 1: Measurement of photovoltaic current-voltage characteristics
IEC 60904-8: 2014 Photovoltaic devices- Part 8: Measurement of spectral responsivity of a photovoltaic (PV) device

检测结果/说明：
Results of Test and additional explanation.

Measurement standards used in this test					
Name	**Number**	**Measuring Range**	**Uncertainty or Accuracy Class or Maximum Permissible Error**	**Name of traceability institution/Certificate No.**	**Due date**
System SourceMeter (Electronic Load)	4082810	100 nA~3 A; (0.1~40) V	U_{rel}=0.005% (k=2)	Shanghai Institute of Metrology and Testing Technology / 2021F11-10-3083069001	2022-03-10
Solar Simulator	2015-006	(300～1200) nm；(800～1200) W/m^2	Spectral Match：(300～310) nm：U_{rel}=7.4% (k=2);(310～400) nm：U_{rel}=6.4% (k=2);(400～1200) nm：U_{rel}=5.5% (k=2);Irradiance Ratio: U_{rel}=1.2% (k=2)	Fujian Metrology Institute/ 21Q2-00682	2022-06-28
WPVS Monocrystalline Silicon Reference Cell	015-2014	(300～1200) nm	U_{rel}=1.3% (k=2)	National Institute of Metrology/ GXgf2021-10725	2023-04-05
Si Photoelectric Detector	Si-2	(200~1100) nm	(300 nm～450 nm) U_{rel}=1.8%～1.3% (k=2)；(450 nm～1000 nm) U_{rel}=1.2%～1.7% (k=2)	National Institute of Metrology/ GXgf2021-10903	2023-03-24
Digital Thermometer	15-B (Q0078.1)	(15～65)℃	U=0.1% (k=2)	Fujian Metrology Institute/21B2-08012	2022-06-22

以下空白
Blank below

10. Device Fabrication and Characterization

Device Fabrication

Organic solar cells were fabricated on glass substrates commercially pre-coated with a layer of indium tin oxide (ITO), constructing the inverted structure of ITO/PEDOT:PSS/Active Layer/Bis-FIMG/Ag. Before fabrication, the substrates were pre-cleaned in an ultrasonic bath of detergent, deionized water, acetone and isopropanol consecutively, and then treated in an ultraviolet ozone generator for 15 min. After that, a thin layer PEDOT:PSS (Baytron P AI4083) was spin coated onto the substrates at 4500 rpm (~20 nm thick) for 30 s and annealed at 150 °C for 20 min. Put the substrates into glovebox, all of the active layer mentioned were spin coated from 16.5 mg/mL (PM6:acceptor = 1:1.2 by wt.) chloroform solution at 2500-3000 rpm for 30 s. Detailed device fabrication conditions were summarized in **Table S3**. After that, a 5 nm Bis-FIMG film was deposited as the cathode buffer layer by the spin-coating of a solution of 1.0 mg/mL Bis-FIMG in methanol. Finally, the Ag (120 nm) electrode was deposited by thermal evaporation, the devices were completed with an active area of 0.06 cm^2.

***J-V* and EQE Measurement**

The current density-voltage (*J-V*) curves of OSCs were performed on a Enlitech SS-F5-3A solar simulator under the condition of AM 1.5 G illumination, whose light intensity was calibrated by a standard Si solar cell at 100 mV cm^{-2}. The EQE data were measured by a Solar Cell Spectral Response Measurement System (RE-R, Enlitech). All of the devices mentioned were tested by a shadow mask with an area of 0.0473 cm^2.

GIWAXS Measurement

GIWAXS measurements were performed in a Xeuss 3.0 SAXS/WAXS system with a wavelength of λ = 1.341 Å at Vacuum Interconnected Nanotech Workstation (Nano-X).

FTPS-EQE Spectra Measurement

The FTPS measurement were performed by using a Bruker Vertex 70 Fourier-transform infrared (FTIR) spectrometer, equipped with a quartz tungsten halogen lamp, a quartz beam-splitter, and an external detector option. A low noise current amplifier (Femto DLPCA-200) was used to amplify the photocurrent produced on the illumination of the photovoltaic devices with light modulated by the FTIR. The output voltage of the current amplifier was fed back into the external detector port of the FTIR. The photocurrent spectrum was collected by FTIR's software.

Electroluminescence (EL) Measurement

The EL signature was recorded with a monochromator and detected with an InGaAs detector. Data collection range is 700-1300 nm.

EQE_{EL} Measurement

EQE_{EL} measurements were performed by applying external voltage sources through the devices from 1V to 3V. A Keithley 2400 SourceMeter was used for supplying voltages and recording injected current, and a Keithley 485 picoammeter was used for measuring the emitted light intensity.

AFM measurement

AFM images were obtained on a VeecoMultiMode atomic force microscopy in the tapping mode.

11. Auxiliary Table

Table S1 UV-vis results of pure acceptors.

Material	UV-vis	
	λ_{max}^{sol} (nm)	λ_{max}^{film} (nm)
L8-BO	732	802
BTP-H2	735	805
L8-BO-F	727	794
L8-BO-Cl	732	799

Table S2 CV results.

Material	$E_{HOMO/LUMO}$ (eV)	E_g^{cv} (eV)
L8-BO	-5.63/-3.90	1.73
BTP-H2	-5.54/-3.88	1.66
L8-BO-F	-5.57/-3.88	1.69
L8-BO-Cl	-5.56/-3.89	1.67

Table S3 Device fabrication conditions.

Active Layer	D:A	Additive	Concentration	Speed	Annealing
PM6:L8-BO	1:1.2	0.25% DIO	16.5 mg/mL	3000 rpm	100°C 8min
PM6:BTP-H2	1:1.2	0.25% DIO	16.5 mg/mL	2500 rpm	80°C 8min
PM6:L8-BO:BTP-H2	1:1.2 (25 wt%)[a]	0.25% DIO	16.5 mg/mL	3000 rpm	80°C 8min
PM6:L8-BO-F	1:1.2	0.25% DIO	16.5 mg/mL	2500 rpm	80°C 8min
PM6:L8-BO-Cl	1:1.2	0.25% DIO	16.5 mg/mL	2500 rpm	80°C 8min

[a] Total D:A wt. ratio is kept as 1:1.2 and the percentage refers to the amount of BTP-H2 incorporated.

Table S4 Device parameters based on PM6:L8-BO-F and PM6:L8-BO-Cl.

Active Layer	V_{oc} (V)	J_{sc} (mA cm^{-2})	J_{cal} (mA cm^{-2}) [a]	FF	PCE (%) [b]
PM6:L8-BO-F	0.929 (0.927±0.001)	23.86 (23.77±0.16)	23.66	77.7 (77.2±0.5)	17.2 (17.0±0.1)
PM6: L8-BO-Cl	0.924 (0.925±0.002)	24.51 (24.30±0.18)	24.11	78.5 (78.0±0.3)	17.7 (17.5±0.2)

[a] Integrated current densities from EQE curves. [b] Average PCEs from 20 devices.

Table S5 Detailed parameters of GIWAXS profiles for the pristine films along with in-plane and out-of-plane directions.

System	In-plane		Out-of-plane			
	Q/Å^{-1}	D/Å	Q /Å^{-1}	D/Å	FWHM	CL/ Å
PM6	0.283	22.2	1.61	3.90	0.328	17.2
L8-BO	0.410	15.3	1.68	3.74	0.351	16.1
BTP-H2	0.408	15.4	1.68	3.74	0.240	23.6

Table S6 Detailed parameters of GIWAXS profiles for the blend films along with in-plane and out-of-plane directions.

System	In-plane		Out-of-plane			
	Q/Å^{-1}	D/Å	Q /Å^{-1}	D/Å	FWHM	CL/ Å
PM6:L8-BO	0.294 0.391	21.4 16.1	1.68	3.74	0.306	18.5
PM6:BTP-H2	0.298 0.393	21.1 16.0	1.68	3.74	0.278	20.3
PM6:L8-BO:BTP-H2	0.302 0.392	20.8 16.0	1.68	3.74	0.296	19.1

Table S7 Comparison of device parameters between this work and references.

Active Layer	V_{oc} (V)	J_{sc} (mA cm^{-2})	FF (%)	PCE (%)	Ref.
PM6:BTP-H2	0.932	25.33	78.5	18.5	Text
PM6:L8-BO:BTP-H2	0.892	26.68	80.7	19.2	Text
PM6:mBzS-4F	0.804	27.72	76.35	17.02	1
PM6:EHBzS-4F	0.825	27.58	70.07	15.94	1
PM6:Y6:ITCPTC	0.861	25.67	78.8	17.42	2
PM6:BTP-eC9:PC71BM	0.845	26.94	79.2	18.03	3
PM6:Y6:PC71BM	0.83	26.6	77.1	17	4
PBTATBT-4f:Y6	0.81	27.25	72.7	16.08	5
PTzBI-dF:y6	0.85	26.33	75.5	16.8	6
SZ5:BPT-4F	0.853	24.8	79.1	16.5	7

SZ5:BPS-4F	0.822	25.4	77.9	16.1	[7]
P2F-Ehp:PCBM:Y6	0.82	26.38	74.8	16.18	[8]
PBQ10:Y6	0.85	25.77	74.6	16.34	[9]
PM6:CH1007:PC71BM	0.822	27.48	75.61	17.08	[10]
D18:Y6-Se	0.839	27.98	75.3	17.7	[11]
PM6:N3:PC71BM	0.841	26.49	78.2	17.42	[12]
PT2:Y6	0.83	26.7	74.4	16.5	[13]
PM6:BTP1O-4Cl-C12	0.91	23.85	78.8	17.1	[14]
PTQ10:BTP-Ph:BTP-Th	0.888	25.2	78.6	17.6	[15]
PM6:Y6:MeIC	0.863	25.4	79.2	17.4	[16]
PM6:Y6-1O:PC71BM	0.9	24.9	78.5	17.6	[17]
PM6:Y6-1O	0.89	23.2	78.3	16.1	[17]
PM6:N3:PC71BM	0.84	26.76	78	17.6	[18]
D18:BTPR:Y6	0.863	27.65	74.6	17.8	[19]
PM6:BO-4Cl:BTP-S2	0.861	27.14	78.04	18.16	[20]
PBDB-TF:AQx-2	0.86	25.38	76.25	16.64	[21]
SZ4:N3	0.848	26	77.4	17.1	[22]
PBTT-F:Y6	0.84	24.8	77.1	16.1	[23]
Pt10:Y6	0.81	26.45	76.3	16.35	[24]
PTQ10:Y6	0.87	24.81	75.1	16.21	[25]
PBDB-TF:BTP-4F-12	0.855	25.3	76	16.4	[26]
PBNT-BDD:Y6	0.88	25.4	72	16.1	[27]
PBDB-TF:BTP-4Cl	0.838	26.7	79	17.7	[28]
PBDB-TF:BTIC-2Cl-Rcf3:PC71ThBM	0.85	25.76	78.1	17.12	[29]
PTQ10:m-BTP-C6Ph	0.883	25.3	79.3	17.7	[30]
PM6:Y18:PC71BM	0.84	26.3	77.4	17.11	[31]
PM6:Y6	0.838	26.71	76.0	17.4	[32]
PL1:N3-Cl-2	0.85	25.62	75.5	16.42	[33]
S1:Y6	0.877	25.402	73.7	16.421	[34]
PM6:M3	0.91	24.03	76.22	16.66	[35]
PM6:BTP-2F-ThCl	0.869	25.38	77.4	17.06	[36]
PM6:N3	0.837	25.81	73.9	15.98	[37]
PM6:Y6:C8-DTC	0.873	26.5	75.61	17.52	[38]
P2F-EHp:BTPTT-4F	0.81	26.68	74.11	16.02	[39]
PM6:BP5T-4F	0.888	24.6	76.3	16.7	[40]
PBDB-TF:BTP-4Cl	0.867	25.4	75	16.5	[41]
PM6:BTP-eC9	0.848	27.12	80.79	18.58	[42]
PM6:CH1007:BT-4BO	0.88	26.9	75.35	17.80	[43]
PM6:L8-BO	0.87	25.72	81.5	18.32	[44]
PB2F:PM6:BTP-eC9	0.863	26.8	80.4	18.6	[45]
PM6:L8-BO	0.89	26.11	80.6	18.74	[46]
PM6:BTP-eC9:PC71BM	0.853	27.6	79.17	18.65	[47]

PB2:BTP-eC9	0.863	26.2	78.4	17.7	48
PBQx-TCl:BTA3:BTP-eC9	0.84	26.9	79.6	18.0	49
PTO3:PM6:BTP-eC9	0.866	26.6	80.3	18.5	50
PBQx-TF:F-BTA3:eC9-2Cl	0.879	26.7	80.9	19.0	51
PM6:BTP-eC9:L8-BO-F	0.853	27.35	80	18.66	52
PTQ10:m-BTP-PhC6:PC71BM	0.869	26.99	80.6	18.89	53
PM6:L8-BO	0.89	26.37	79.94	18.77	54
PM6:BTP-eC9	0.85	28.18	76.46	18.27	55
PM6:BTP-eC9:HDO-4Cl	0.866	27.05	80.51	18.86	56
D18-Cl:G19:Y60	0.871	27.36	77.72	18.53	57
PM6:BTP-T-3Cl:BTP-4Cl-BO	0.857	27.38	77.73	18.21	58
PM6:BTP-eC11:BTP-S2	0.872	26.62	79.0	18.31	59
PM6:BTP-eC9:BTP-S2	0.878	26.78	79.44	18.66	60
PM6:AC9	0.871	26.75	79.0	18.43	61

12. References

1. F. Qi, K. Jiang, F. Lin, Z. Wu, H. Zhang, W. Gao, Y. Li, Z. Cai, H. Y. Woo, Z. Zhu, A. K. Y. Jen, *ACS Energy Lett.*, 2020, **6**, 9.
2. R. Ma, T. Liu, Z. Luo, K. Gao, K. Chen, G. Zhang, W. Gao, Y. Xiao, T.-K. Lau, Q. Fan, Y. Chen, L.-K. Ma, H. Sun, G. Cai, T. Yang, X. Lu, E. Wang, C. Yang, A. K. Y. Jen and H. Yan, *ACS Energy Lett.*, 2020, **5**, 2711-2720.
3. Y. Lin, Y. Firdaus, F. H. Isikgor, M. I. Nugraha, E. Yengel, G. T. Harrison, R. Hallani, A. El-Labban, H. Faber, C. Ma, X. Zheng, A. Subbiah, C. T. Howells, O. M. Bakr, I. McCulloch, S. D. Wolf, L. Tsetseris and T. D. Anthopoulos, *ACS Energy Lett.*, 2020, **5**, 2935-2944.
4. Q. Li, L.-M. Wang, S. Liu, L. Guo, S. Dong, G. Ma, Z. Cao, X. Zhan, X. Gu, T. Zhu, Y.-P. Cai and F. Huang, *ACS Energy Lett.*, 2020, **5**, 3637-3646.
5. L.-W. Feng, J. Chen, S. Mukherjee, V. K. Sangwan, W. Huang, Y. Chen, D. Zheng, J. W. Strzalka, G. Wang, M. C. Hersam, D. DeLongchamp, A. Facchetti and T. J. Marks, *ACS Energy Lett.*, 2020, **5**, 1780-1787.
6. B. Fan, M. Li, D. Zhang, W. Zhong, L. Ying, Z. Zeng, K. An, Z. Huang, L. Shi, G. C. Bazan, F. Huang and Y. Cao, *ACS Energy Lett.*, 2020, **5**, 2087-2094.
7. G. Chai, J. Zhang, M. Pan, Z. Wang, J. Yu, J. Liang, H. Yu, Y. Chen, A. Shang, X. Liu, F. Bai, R. Ma, Y. Chang, S. Luo, A. Zeng, H. Zhou, K. Chen, F. Gao, H. Ade and H. Yan, *ACS Energy Lett.*, 2020, **5**, 3415-3425.
8. B. Fan, Z. Zeng, W. Zhong, L. Ying, D. Zhang, M. Li, F. Peng, N. Li, F. Huang and Y. Cao, *ACS Energy Lett.*, 2019, **4**, 2466-2472.
9. C. Sun, F. Pan, B. Qiu, S. Qin, S. Chen, Z. Shang, L. Meng, C. Yang and Y. Li, *Chem. Mater.*, 2020, **32**, 3254-3261.
10. F. Lin, K. Jiang, W. Kaminsky, Z. Zhu and A. K. Jen, *J. Am. Chem. Soc.*, 2020,

142, 15246-15251.
11. Z. Zhang, Y. Li, G. Cai, Y. Zhang, X. Lu and Y. Lin, *J. Am. Chem. Soc.*, 2020, **142**, 18741-18745.
12. K. Jiang, J. Zhang, Z. Peng, F. Lin, S. Wu, Z. Li, Y. Chen, H. Yan, H. Ade, Z. Zhu and A. K. Jen, *Nat. Commun.*, 2021, **12**, 468.
13. K. Weng, L. Ye, L. Zhu, J. Xu, J. Zhou, X. Feng, G. Lu, S. Tan, F. Liu and Y. Sun, *Nat. Commun.*, 2020, **11**, 2855.
14. Y. Chen, R. Ma, T. Liu, Y. Xiao, H. K. Kim, J. Zhang, C. Ma, H. Sun, F. Bai, X. Guo, K. S. Wong, X. Lu and H. Yan, *Adv. Energy Mater.*, 2021, **11**.
15. Y. Chang, J. Zhang, Y. Chen, G. Chai, X. Xu, L. Yu, R. Ma, H. Yu, T. Liu, P. Liu, Q. Peng and H. Yan, *Adv. Energy Mater.*, 2021, DOI: 10.1002/aenm.202100079.
16. X. Ma, J. Wang, J. Gao, Z. Hu, C. Xu, X. Zhang and F. Zhang, *Adv. Energy Mater.*, 2020, DOI: 10.1002/aenm.202001404.
17. Y. Chen, F. Bai, Z. Peng, L. Zhu, J. Zhang, X. Zou, Y. Qin, H. K. Kim, J. Yuan, L. K. Ma, J. Zhang, H. Yu, P. C. Y. Chow, F. Huang, Y. Zou, H. Ade, F. Liu and H. Yan, *Adv. Energy Mater.*, 2020, **11**.
18. Y. Qin, Y. Xu, Z. Peng, J. Hou and H. Ade, *Adv. Funct. Mater.*, 2020, **30**.
19. Y. Zhang, G. Cai, Y. Li, Z. Zhang, T. Li, X. Zuo, X. Lu and Y. Lin, *Adv. Mater.*, 2021, DOI: 10.1002/adma.202008134, 2008134.
20. L. Zhan, S. Li, X. Xia, Y. Li, X. Lu, L. Zuo, M. Shi and H. Chen, *Adv. Mater.*, 2021, **33**, 2007231.
21. Z. Zhou, W. Liu, G. Zhou, M. Zhang, D. Qian, J. Zhang, S. Chen, S. Xu, C. Yang, F. Gao, H. Zhu, F. Liu and X. Zhu, *Adv. Mater.*, 2020, **32**, 1906324.
22. J. Liang, M. Pan, G. Chai, Z. Peng, J. Zhang, S. Luo, Q. Han, Y. Chen, A. Shang, F. Bai, Y. Xu, H. Yu, J. Y. L. Lai, Q. Chen, M. Zhang, H. Ade and H. Yan, *Adv. Mater.*, 2020, **32**, 2003500.
23. P. Chao, H. Chen, Y. Zhu, H. Lai, D. Mo, N. Zheng, X. Chang, H. Meng and F. He, *Adv. Mater.*, 2020, **32**, 1907059.
24. X. Xu, K. Feng, Z. Bi, W. Ma, G. Zhang and Q. Peng, *Adv. Mater.*, 2019, **31**, e1901872.
25. C. Sun, F. Pan, S. Chen, R. Wang, R. Sun, Z. Shang, B. Qiu, J. Min, M. Lv, L. Meng, C. Zhang, M. Xiao, C. Yang and Y. Li, *Adv. Mater.*, 2019, **31**, 1905480.
26. L. Hong, H. Yao, Z. Wu, Y. Cui, T. Zhang, Y. Xu, R. Yu, Q. Liao, B. Gao, K. Xian, H. Y. Woo, Z. Ge and J. Hou, *Adv. Mater.*, 2019, **31**, 1903441.
27. S. Pang, Z. Wang, X. Yuan, L. Pan, W. Deng, H. Tang, H. Wu, S. Chen, C. Duan, F. Huang and Y. Cao, *Angew. Chem. Int. Ed.*, 2021, **60**, 8813-8817.
28. L. Ma, H. Yao, J. Wang, Y. Xu, M. Gao, Y. Zu, Y. Cui, S. Zhang, L. Ye and J. Hou, *Angew. Chem. Int. Ed.*, 2021, DOI: 10.1002/anie.202102622.
29. X. Huang, J. Oh, Y. Cheng, B. Huang, S. Ding, Q. He, F. Wu, C. Yang, L. Chen and Y. Chen, *J. Mater. Chem. A*, 2021, **9**, 5711-5719.
30. G. Chai, Y. Chang, J. Zhang, X. Xu, L. Yu, X. Zou, X. Li, Y. Chen, S. Luo, B.

Liu, F. Bai, Z. Luo, H. Yu, J. Liang, T. Liu, K. S. Wong, H. Zhou, Q. Peng and H. Yan, *Energy Environ. Sci.*, 2021, DOI: 10.1039/d0ee03506h.

31. C. Zhu, J. Yuan, F. Cai, L. Meng, H. Zhang, H. Chen, J. Li, B. Qiu, H. Peng, S. Chen, Y. Hu, C. Yang, F. Gao, Y. Zou and Y. Li, *Energy Environ. Sci.*, 2020, DOI: 10.1039/d0ee00862a.
32. L. Ye, Y. Cai, C. Li, L. Zhu, J. Xu, K. Weng, K. Zhang, M. Huang, M. Zeng, T. Li, E. Zhou, S. Tan, X. Hao, Y. Yi, F. Liu, Z. Wang, X. Zhan and Y. Sun, *Energy Environ. Sci.*, 2020, **13**, 5117-5125.
33. X. Li, I. Angunawela, Y. Chang, J. Zhou, H. Huang, L. Zhong, A. Liebman-Pelaez, C. Zhu, L. Meng, Z. Xie, H. Ade, H. Yan and Y. Li, *Energy Environ. Sci.*, 2020, **13**, 5028-5038.
34. H. Sun, T. Liu, J. Yu, T.-K. Lau, G. Zhang, Y. Zhang, M. Su, Y. Tang, R. Ma, B. Liu, J. Liang, K. Feng, X. Lu, X. Guo, F. Gao and H. Yan, *Energy Environ. Sci.*, 2019, **12**, 3328-3337.
35. Y. Ma, M. Zhang, S. Wan, P. Yin, P. Wang, D. Cai, F. Liu and Q. Zheng, *Joule*, 2021, **5**, 197-209.
36. Z. Luo, R. Ma, T. Liu, J. Yu, Y. Xiao, R. Sun, G. Xie, J. Yuan, Y. Chen, K. Chen, G. Chai, H. Sun, J. Min, J. Zhang, Y. Zou, C. Yang, X. Lu, F. Gao and H. Yan, *Joule*, 2020, DOI: 10.1016/j.joule.2020.03.023.
37. K. Jiang, Q. Wei, J. Y. L. Lai, Z. Peng, H. K. Kim, J. Yuan, L. Ye, H. Ade, Y. Zou and H. Yan, *Joule*, 2019, **3**, 3020-3033.
38. T. Liu, R. Ma, Z. Luo, Y. Guo, G. Zhang, Y. Xiao, T. Yang, Y. Chen, G. Li, Y. Yi, X. Lu, H. Yan and B. Tang, *Energy Environ. Sci.*, 2020, **13**, 2115-2123.
39. B. Fan, D. Zhang, M. Li, W. Zhong, Z. Zeng, L. Ying, F. Huang and Y. Cao, *Sci. China Chem.*, 2019, **62**, 746-752.
40. W. Gao, H. Fu, Y. Li, F. Lin, R. Sun, Z. Wu, X. Wu, C. Zhong, J. Min, J. Luo, H. Y. Woo, Z. Zhu and A. K. Y. Jen, *Adv. Energy Mater.*, 2020, **11**.
41. Y. Cui, H. Yao, J. Zhang, T. Zhang, Y. Wang, L. Hong, K. Xian, B. Xu, S. Zhang, J. Peng, Z. Wei, F. Gao and J. Hou, *Nat. Commun.*, 2019, **10**, 2515.
42. X. Xiong, X. Xue, M. Zhang, T. Hao, Z. Han, Y. Sun, Y. Zhang, F. Liu, S. Pei and L. Zhu, *ACS Energy Lett.*, 2021, **6**, 3582-3589.
43. B. Fan, W. Gao, Y. Wang, W. Zhong, F. Lin, W. J. Li, F. Huang, K.-M. Yu and A. K. Y. Jen, *ACS Energy Lett.*, 2021, **6**, 3522-3529.
44. C. Li, J. Zhou, J. Song, J. Xu, H. Zhang, X. Zhang, J. Guo, L. Zhu, D. Wei, G. Han, J. Min, Y. Zhang, Z. Xie, Y. Yi, H. Yan, F. Gao, F. Liu and Y. Sun, *Nat. Energy*, 2021, DOI: 10.1038/s41560-021-00820-x.
45. T. Zhang, C. An, P. Bi, Q. Lv, J. Qin, L. Hong, Y. Cui, S. Zhang and J. Hou, *Adv. Energy Mater.*, 2021, **11**.
46. X. Xu, L. Yu, H. Meng, L. Dai, H. Yan, R. Li and Q. Peng, *Adv. Funct. Mater.*, 2021, DOI: 10.1002/adfm.202108797.
47. R. Sun, T. Wang, Y. Wu, M. Zhang, Y. Ma, Z. Xiao, G. Lu, L. Ding, Q. Zheng, C. J. Brabec, Y. Li and J. Min, *Adv. Funct. Mater.*, 2021, DOI:

10.1002/adfm.202106846.
48. T. Zhang, C. An, Y. Cui, J. Zhang, P. Bi, C. Yang, S. Zhang and J. Hou, *Adv. Mater.*, 2021, DOI: 10.1002/adma.202105803, e2105803.
49. Y. Xu, Y. Cui, H. Yao, T. Zhang, J. Zhang, L. Ma, J. Wang, Z. Wei and J. Hou, *Adv. Mater.*, 2021, **33**, e2101090.
50. L. Hong, H. Yao, Y. Cui, P. Bi, T. Zhang, Y. Cheng, Y. Zu, J. Qin, R. Yu, Z. Ge and J. Hou, *Adv. Mater.*, 2021, DOI: 10.1002/adma.202103091, e2103091.
51. Y. Cui, Y. Xu, H. Yao, P. Bi, L. Hong, J. Zhang, Y. Zu, T. Zhang, J. Qin, J. Ren, Z. Chen, C. He, X. Hao, Z. Wei and J. Hou, *Adv. Mater.*, 2021, DOI: 10.1002/adma.202102420, 2102420.
52. Y. Cai, Y. Li, R. Wang, H. Wu, Z. Chen, J. Zhang, Z. Ma, X. Hao, Y. Zhao, C. Zhang, F. Huang and Y. Sun, *Adv. Mater.*, 2021, DOI: 10.1002/adma.202101733, e2101733.
53. S. Bao, H. Yang, H. Fan, J. Zhang, Z. Wei, C. Cui and Y. Li, *Adv. Mater.*, 2021, DOI: 10.1002/adma.202105301.
54. H. Meng, C. Liao, M. Deng, X. Xu, L. Yu and Q. Peng, *Angew. Chem. Int. Ed.*, 2021, **60**, 22554-22561.
55. Y. Li, J. Ding, C. Liang, X. Zhang, J. Zhang, D. S. Jakob, B. Wang, X. Li, H. Zhang, L. Li, Y. Yang, G. Zhang, X. Zhang, W. Du, X. Liu, Y. Zhang, Y. Zhang, X. Xu, X. Qiu and H. Zhou, *Joule*, 2021, DOI: 10.1016/j.joule.2021.09.001.
56. P. Bi, S. Zhang, Z. Chen, Y. Xu, Y. Cui, T. Zhang, J. Ren, J. Qin, L. Hong, X. Hao and J. Hou, *Joule*, 2021, DOI: 10.1016/j.joule.2021.06.020.
57. Z. Chen, W. Song, K. Yu, J. Ge, J. Zhang, L. Xie, R. Peng and Z. Ge, *Joule*, 2021, DOI: 10.1016/j.joule.2021.06.017.
58. Y. Pan, X. Zheng, J. Guo, Z. Chen, S. Li, C. He, S. Ye, X. Xia, S. Wang, X. Lu, H. Zhu, J. Min, L. Zuo, M. Shi and H. Chen, *Adv. Funct. Mater.*, 2021, DOI: 10.1002/adfm.202108614.
59. L. Zuo, S. B. Jo, Y. Li, Y. Meng, R. J. Stoddard, Y. Liu, F. Lin, X. Shi, F. Liu, H. W. Hillhouse, D. S. Ginger, H. Chen and A. K. Jen, *Nat. Nanotechnol.*, 2022, **17**, 53-60.
60. Y. Li, Y. Guo, Z. Chen, L. Zhan, C. He, Z. Bi, N. Yao, S. Li, G. Zhou, Y. Yi, Y. Yang, H. Zhu, W. Ma, F. Gao, F. Zhang, L. Zuo and H. Chen, *Energy Environ. Sci.*, 2022, DOI: 10.1039/d1ee02977k.
61. C. He, Z. Bi, Z. Chen, J. Guo, X. Xia, X. Lu, J. Min, H. Zhu, W. Ma, L. Zuo and H. Chen, *Adv. Funct. Mater.*, 2022, DOI: 10.1002/adfm.202112511.